

An extension of the Budyko model with iceline

Honors Student: Monika Morasse¹

Thesis Advisor: Anca Rădulescu²

¹ *Department of Mathematics, SUNY New Paltz*

² *Department of Mathematics, SUNY New Paltz*

Abstract: Budyko's energy model is a historic system of differential equations, capturing the effect of the water albedo on climate trends. This has been analyzed by many researchers and is the basis of our work. The position of the Earth's iceline, and its coupling with temperature, play a very important role in determining long term climate patterns (which range between extremes from a water covered to an ice covered Earth). We built upon established results of Budyko and others, and additionally studied how two important system parameters related to water purity (the glacier forming temperature, T_c , and the water albedo, α_w) may impact the long-term climatic outcome. We found that perturbing either of these parameters had significant global effects. Moreover, these effects were enhanced when occurring in combination, and even more so when in the presence of an elevated greenhouse effect.

Keywords: Mathematics; climate modeling; water albedo; freezing temperature; greenhouse effect; dynamical systems; stability of equilibria; bifurcation analysis.

1 Introduction

Earth's climate is constantly changing. It exhibits patterns of fluctuations and cycles, some of which occur naturally, as part of the intrinsic dynamics of a self-regulating system. There is, however, increasing evidence that some climate trends are triggered by external, human-induced factors. Over the past decade, the idea that the Earth's climate may be significantly and potentially irreversibly altered by human activities has become a scientifically documented and accepted theory. Climate change is the subject of ample data-driven studies and of massive modeling efforts. These aim to understand which factors and human activities have the most detrimental effect on the system's dynamics and regulation, and predict whether this regulation can be restored if some of the negative impact is eliminated.

One of the primary effects studied in conjunction with climate change is the green-house effect. As the density of CO_2 (and of other similar gases) has been gradually increasing in the Earth's atmosphere over the past century, the annual average Earth temperature has been steadily climbing. This correlation is not accidental: CO_2 accumulating in the atmosphere prevents the light reflected by the Earth surface from escaping back into space, hence the trapped solar radiation leads to the consistent increase in Earth average temperature.

There are now many mathematical models based on global patterns in the ocean and atmosphere, that can be used to support and understand empirically patterns displaying the green-house effect. One of the first pure theoretical investigations was Budyko's model, an energy balance model (EBM) that provides a broad brushstroke view of the dynamics of climate based on the interaction of major climate components (incoming solar radiation, planetary albedo).

Budyko's EBM captures in basic and beautifully simple form the ice-albedo feedback mechanism: the more snow and ice there is, the more solar radiation is reflected back into space. When this occurs, Earth grows colder and this results in more snow.

The model assumes the annual average Earth surface temperature T (in $^{\circ}C$) to be constant around latitude circles, and symmetric across the equator. Then represents $T = T(t, y)$ as a function of time t and of the sine of the latitude ($y = \sin(\theta)$):

$$R \frac{\partial T}{\partial t} = Qs(y)(1 - \alpha(y, \eta)) - (A + BT) + C(\bar{T} - T) \quad (1)$$

where \bar{T} is the mean temperature over all latitudes:

$$\bar{T}(t) = \int_0^1 T(t, y) dy$$

The change in temperature is primarily driven by the amount of incoming solar energy (insolation). The proportion of solar energy reflected back into space is determined by the Earth's albedo α . In reality the albedo is a local measure, that differs between land and water, and even with local physical properties of these. For simplification, the model assumes that the Earth is covered in water (extrapolating the fact that the planetary ocean covers a significantly large proportion of the Earth surface). Then the albedo only depends on latitude (via the position with respect to the fixed iceline position $\eta \in [0, 1]$), and can only take two discrete values: that of water (below the iceline), and that of ice (above the iceline):

$$\alpha(y, \eta) = \begin{cases} \alpha_w, & \text{if } y < \eta \\ \alpha_s, & \text{if } y > \eta \end{cases}$$

More radiation is reflected for ice than water, hence $\alpha_s > \alpha_w$. Altogether, the average annual rate at which solar energy is absorbed by the Earth's surface can be then expressed as $Qs(y)(1 - \alpha(y, \eta))$, where Q is the annual mean insolation, and $s(y)$ represents the distribution of this insolation over all latitudes.

The second term represents the energy that leaves the system via outgoing longwave radiation (OLR), which decreases with the green-house effect (greenhouse gasses in the atmosphere block radiation from escaping). The term is represented as a linear approximation, in which lower values of the parameters A and B are tied to higher amounts of atmospheric CO_2 . The final term represents heat transfer between latitudes (also known as “convection”).

Over time, many researchers have improved the Budyko framework with more specific interactions. Our work builds upon a two-dimensional extension constructed and studied by McGehee and Widiasih [9] as well as by McGehee and Walsh [6]. The model realistically introduces a moving iceline η , and reproduces the coupled behavior of the temperature-iceline system.

If we assumed, as in Budyko’s model, that the ice line was stationary, the average temperature across that iceline would be $T_c \sim -10^\circ C$ (the approximate glacier formation temperature). In reality, however, the stationary assumption is not realistic [?]: if the temperature T at the iceline latitude $y = \eta$ is greater than T_c , the ice line will recede towards the pole ($\eta = 1$) and if the temperature is below T_c , the iceline will advance towards the equator. To capture this effect, Widiasih [?] introduced an additional equation that couples iceline dynamics with that of temperature. The rate of change of the ice line is considered proportional to the difference between the equilibrium temperature profile and the glacier-forming temperature T_c (with a very large time scale $1/\varepsilon$ reflecting glacier dynamics).

$$\frac{d\eta}{dt} = \varepsilon(T_\eta^*(\eta) - T_c) \quad (2)$$

Broadly speaking, this coupling captures the idea that, when ice is melting, more water is exposed, absorbing more of the Sun’s energy. This causes the surface to warm up, and more ice to melt. Conversely, when the ice is advancing, more of the Sun’s energy is reflected, causing the surface to cool, causing more ice to form.

Via a Legendre expansion and change of variables to find a two dimensional invariant subspace, McGehee and Widiasih obtained a simpler system of two coupled differential equations [?]:

$$\begin{aligned} \frac{d\eta}{dt} &= \varepsilon \left[w + \frac{Qs_2}{2} \left(1 - \frac{\alpha_w + \alpha_s}{2} \right) \left(\frac{3\eta^2 - 1}{B + C} \right) - T_c \right] \\ R \frac{dw}{dt} &= Q \left(1 - \frac{\alpha_w + \alpha_s}{2} \right) - A + \frac{QC}{B + C} (\alpha_s - \alpha_w) \left(\eta - \frac{1}{2} + \frac{s_2}{2} (\eta^3 - \eta) \right) - Bw - \Omega \frac{d\eta}{dt}. \end{aligned} \quad (3)$$

where a quadratic approximation was used for the insolation distribution: $s(y) = 1 + \frac{s_2}{2}(3y^2 - 1)$, and Ω represents the amount of energy required to melt a square meter of ice. Note that the iceline, η , is measured within the range of 0 to 1. Once the iceline reaches the equator, $\eta = 0$, or the pole, $\eta = 1$, the equations stop accurately describing the dynamics, and the system is governed by new regulatory drives, corresponding to an ice covered or water covered Earth, respectively.

This system was studied by McGehee, Walsh and Widiasih, with a combination of analytical and numerical computations. It was established that, for a parameter range compatible with current satellite measured-values, there are two locally stable equilibria (one with high iceline, and one in the nonviable negative η interval), and a saddle (corresponding to a lower η), as shown in Figure 1a. Subsequently, the Earth may stabilize to long term steady state with small ice caps, or may end up completely covered in either ice or water. One direction of the analysis targeted the dependence of the long-term behavior of the system on the level of atmospheric greenhouse gasses (as captured by the parameter A). Numerical simulations revealed a saddle-node bifurcation, suggesting that low A values (high greenhouse effect) may lead to a water covered Earth, high A values (low greenhouse effect) may lead to an ice covered Earth, while intermediate A values, compatible to current measures values, fall in a range where a steady high iceline is possible (see Figure 1b).

In this paper, we will build upon this system and focus in more detail on two additional aspects that may contribute to the temperature-iceline coupling – and which were not included in the original

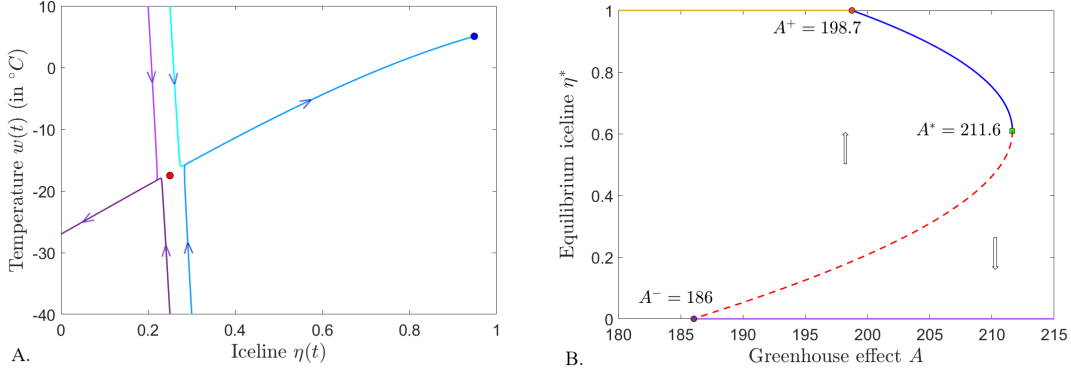


Figure 1: **dynamic behavior of the original system.** **A.** Phase plane showing the three co-existing equilibria, for $A = 202$: a locally stable equilibrium (blue dot) at $(\eta^*, w^*) \sim (0.95, 5)$; a saddle equilibrium (red dot) at $(\eta^*, w^*) \sim (0.25, -17.5)$, and a second locally stable equilibrium at $(\eta^*, w^*) \sim (0.95, 5)$ (not shown in the range). **B.** Bifurcation diagram with respect to A . The high iceline stable equilibrium branch collides with the pole $\eta = 1$ at $A^- = 198.7$, and with the saddle equilibrium branch at the saddle node bifurcation point $A^* = 211.6$. The water covered Earth prediction is represented by an orange line at $\eta = 1$, and the ice-covered Earth is shown as a purple line at $\eta = 0$. The other parameters were fixed to the nominal values in Table 1, with $\alpha = 0.32$ and $T_c = -10^{\circ}\text{C}$.

model, in favor of simplicity. One aspect relates to the effect of clouds. Recall that planetary albedo is what percent of the sunshine is reflected back into space, and is captured in our current model by the parameters α_w (above water surfaces) and α_s (above ice). Globally the albedo is ruled by clouds, the formation of which is temperature dependent. The higher the temperature w , the warmer the sea surface is, hence the higher evaporation and the more water (higher cloud cover C_c) in the atmosphere [4]. Climate studies have documented lagged correlations between the two, in a variety of settings [5, 7]. There have been attempts to quantify this relationship, at different spatial and temporal scales. A study by Oreopoulos and Davies [7] for example, suggests that the variation in albedo due to temperature changes may depend linearly on the change in cloud cover with surface temperature and on local cloud albedo changes (i.e., changes in the albedo of each cloud pixel at ISCCP resolution). However, determining the influence of surface temperature on water albedo in a planetary ocean setting is not trivial, since the coupling appears to also involve strong feedback (cloud albedo contributes to ocean temperature regulation, at a local scale). This makes it harder to separate and quantitatively infer the direct influence of one onto the other simply from data. A model setting can help us set testable predictions with respect to the effect of clouds on the overall systemic dynamics.

The second aspect relates to water quality, and its potential effect on the system’s dynamics – via its impact not only on the water albedo, but also on its freezing point. Due to the nature of the model, we will only discuss this in terms of global changes to water quality. We consider the potential of water pollution to produce changes to the chemistry of the water and to aquatic vegetation, which may in turn alter the absorption index, hence also the albedo. We also consider the fact that most water contaminants (such as industrial pollutants, but also natural salt) are not retained in ice when water freezes. Hence lower ice lines (larger ice caps) lead to higher concentrations in water contaminants and potentially lower freezing points, slowing down further ice formation, and adding a regulatory mechanism against the progression to a completely frozen Earth.

The rest of the paper is organized as follows. In Section 2, we describe the new aspects that we

incorporated into the existing Budyko model with coupled iceline, and the modeling steps taken to address them. In Section 3, we present and contextualize the results of our simulations. In Section 4, we compare our predictions with those of the original model, as well as with realistic predictions based on climate data. Finally, in Section ??, we describe the limitations of our model, and potential ideas to pursue in future work.

2 Modeling methods

We will be studying the Budyko model with coupled iceline, as described in Equations (1)- (2), with parameter values and ranges specifies in Table 1. Known consequences of water pollution include physical and chemical changes. Among the known and well-studied effects are changes in freezing point in conjunction with certain contaminants, and changes in optical properties (reflectiveness of the water surface). In the case of our model, these properties are respectively captured by two parameters: T_c , the water temperature of glacier formation, and α_w , the water albedo. To incorporate potential effects of water contamination on the evolution of the temperature-iceline system, we allowed these parameters to vary within the ranges specified in the table, while keeping the other parameters fixed to the nominal table values. We will examine the dependence on parameters via bifurcation diagrams, computed numerically with the Matcont software (unless otherwise specified).

Parameter	Value	Units	Definition
Q	343	W/m^2	“solar constant”
s_2	-0.482	Dimensionless	
A	[190,212]	W/m^2	amount of carbon in the air; affects OLR
B	1.9	$W/m^2 \text{ } ^\circ C$	amount of carbon in the air; affects OLR
D	3.04	$W/m^2 \text{ } ^\circ C$	positive constant
R	4×10^9	$J/m^2 \text{ } ^\circ C$	time constant
α_w	[0.1,0.5]	Dimensionless	water albedo
α_s	0.62	Dimensionless	ice albedo
T_c	[-15,-5]	$^\circ C$	glacier forming temperature
Ω	$1.5 \cdot 10^{11}$	J/m^2	amount of energy required to melt a square meter of ice
ε	$3.9 \cdot 10^{-13}$		time constant

Table 1: **Model parameter values and units**, as per the original references.

As in our previous analysis [2], we performed a change of scale (e.i., a change in units of our time constants). Using a millennium (10^3 years $\sim 3.16 \times 10^{10}$ seconds) as our time unit, the original values of our time constants $R = 4 \cdot 10^9$, $\Omega = 1.5 \cdot 10^{11}$, $\varepsilon = 3.9 \cdot 10^{-13}$ become $R = 0.1266$, $\Omega = 0.474$, $\varepsilon = 0.01264$. All simulations are performed with these transformed values, hence the convergence kinetics in the simulations occurs on a time scale measured in thousands of years.

Modeling the effects of varying the freezing point T_c . In the original model, the temperature T_c where glaciers form is considered as a fixed parameter. However, as pointed in the Introduction, the freezing temperature of water is known to depend on the water purity. Some contaminants (among which salt, one of the main components in planetary ocean water) have the ability to significantly lower the freezing point. Hence we deem it important to investigate the effects on the system of changing the value of T_c around its nominal value in Table 1. For simplicity, we assume that the planetary water is well stirred, so the water quality is the same everywhere.

Modeling the effects of varying the albedo α_w . In the original model, the water albedo is considered a fixed parameter. However, there is ample evidence that the albedo varies widely with circumstances (such as presence of clouds), and that these variations can have significant contributions to the iceline system dynamics. We study the effects to the long-term prognosis of the system of perturbations in the water albedo values α_w around the nominal value in Table 1. Intrinsically, the albedo is higher up north, where the surface is covered in ice. However, the sub exposure is dramatically reduced as one gets close to the poles (winters are longer). Therefore, under normal circumstances, ice contributes less to the total planetary albedo (does not reflect much sunshine in an average year) Hence, in our analysis, we will keep α_s fixed to its table nominal value.

Modeling how greenhouse effects modulate the effects of salinity and albedo. We will first perturb T_c and α_w independently, to observe the effects of each factor in isolation. We then aim to study their combined contributions, as well as how these are modulated by other aspects significant to the system, such as the greenhouse effect (captured by the parameter A). The system’s sensitivity and dynamic changes in response to perturbations in the greenhouse effect A have been abundantly studied by McGehee and Walsh [8]. In our analysis, we will focus on understanding whether the impact of changing T_c and α_w on dynamics is increased if the water pollution is accompanied by an increased greenhouse effect (lower A).

3 Results

3.1 Dependence of system dynamics on water quality

For this analysis, our key parameters are T_c (the glacier forming water temperature) and α_w (the water albedo), since they directly depend on water quality. In this section, to fix our ideas, we allowed the system to operate under a moderate amount of atmospheric carbon, specified by $A = 202$. In Section 3.2, we study how perturbations to higher or lower greenhouse gases may affect the behavior of the system. For all simulations, all other parameters were fixed to their nominal values in Table 1.

3.1.1 Dependence on glacier forming temperature T_c

We studied changes in the behavior of the system in response to perturbations to the freezing temperature T_c around its baseline value $T_c = -10^\circ\text{C}$, reflecting the effects of water contaminants (including salt) on the chemical potential of the resulting fluid to freeze. All other parameters were fixed as specified at the start of Section 3.1. In addition, the water albedo was fixed to its baseline value $\alpha_w = 0.32$.

Figure 2 shows the behavior of the system’s equilibrium under perturbations to T_c in the form of a bifurcation diagram. A locally stable and a saddle branch of the steady state meet at a saddle node point at $T_c^* = -4.92$. In addition, notice that the stable (blue) equilibrium branch hits the top $\eta = 1$ iceline bound for $T_c^+ = -11.75$, and that the unstable (dotted red) branch hits the bottom $\eta = 0$ iceline bound at $T_c^- = -18.4$. Hence the system only has access to the stable equilibrium (η^*, w^*) for values of T_c in the interval $[-11.75, -4.92]$, and otherwise approaches asymptotically either a water-covered Earth (for low values of T_c), or an ice-covered Earth (for high values of T_c).

More specifically, if the freezing temperature T_c is higher than the saddle node bifurcation value $T_c^* = -4.92$, the long-term result is an ice-covered Earth with long-term temperature lower than -20°C (represented in the figure by the purple line).

As T_c is lowered past the bifurcation point, the fate of the system is determined by its initial state. A combination of high enough iceline and temperature places the system in the attraction basin of the stable equilibrium, and the result is a partly ice-covered Earth (blue curve), with

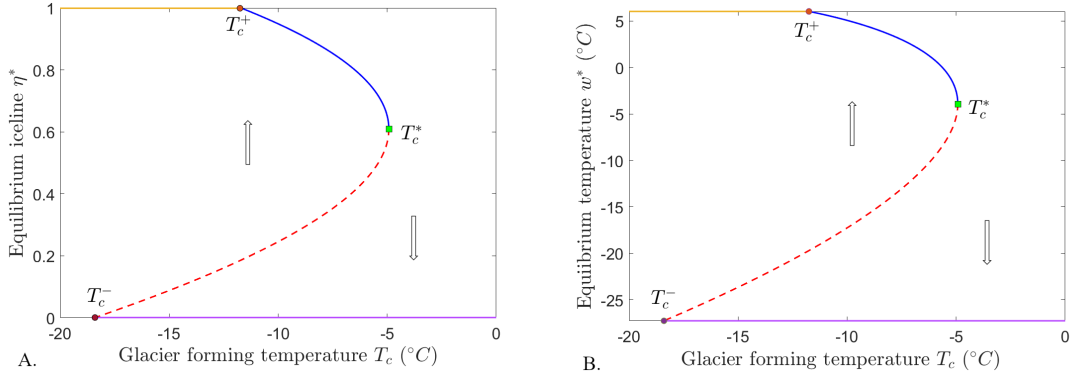


Figure 2: **Bifurcation of the system’s equilibrium with respect to the glacier forming temperature T_c .** The panels show the evolution of the iceline component η (left) and of the temperature component T (right) of the equilibrium, as the parameter T_c changes. A locally stable branch (blue solid curve) and a saddle branch of the equilibrium (red dotted curve) collide at a saddle node bifurcation point at $T_c = T_c^*$, marked as a green square. The point where the stable equilibrium hits the upper iceline bound (at $T_c = T_c^+$) is marked with a brown dot. The iceline $\eta = 1$ (in the left panel) and the corresponding temperature ($w = w^+$, in the right panel) are marked as orange curves for $T_c < T_c^+$, since this state now attracts all initial conditions in the region marked by the upward arrow. The point where the saddle equilibrium hits the lower iceline bound (at $T_c = T_c^-$) is marked with a purple dot. The iceline $\eta = 0$ (in the left panel) and the corresponding temperature ($w = w^-$, in the right panel) are marked as violet curves for $T_c > T_c^-$, since this state now attracts all initial conditions in the region marked by the downward arrow.

equilibrium iceline and temperature increasing with lowering T_c . If the initial state is not in this attraction basin, the result is an ice-covered Earth (purple line).

If one continues to lower T_c past the value $T_c^+ = -11.75^\circ\text{C}$, the stable equilibrium is no longer reachable within the biological range (since $\eta^* > 1$), and all initial conditions within its attraction basin will converge in reality to an ice-free Earth, with a high average temperature over 5°C (orange line). The other initial conditions converge to the ice-covered Earth (purple line). Lowering T_c beyond the value $T_c^- = -18.4^\circ\text{C}$ will seal the long-term fate of the system to the ice-free scenario, independently on the starting conditions.

Recall that the current measured value of T_c is approximately -10°C , placing the system within the interval $[T_c^+, T_c^*]$, and predicting an equilibrium with iceline $\eta^* = 0.95$ (small ice caps) and temperature $w^* = 4.95^\circ\text{C}$, corresponding roughly to our current living conditions. Perturbations to higher T_c values produce a smooth decline in the iceline, until the bifurcation value T_c^* marks the crash to the ice-covered Earth. Perturbations to lower T_c values produce a smooth retraction of the iceline, until the value T_c^+ marks the transition to an ice-free Earth. Both these extreme scenarios are relative well-separated from our current situation ($T_c = -10$), since the values of T_c^* and T_c^+ are far enough to not be reachable via small perturbations in water quality. However, it is possible that changes in other system parameters (such as the water albedo α_w , or the green house effects A) could change the position and shape of this bifurcation scheme to the point where these scenarios may become dangerously within reach. In the next sections, we investigate whether this may be the case.

3.1.2 Dependence on water albedo α_w

We next studied changes in the behavior of the system in response to independently perturbing the water albedo parameter around its baseline value $\alpha_w = 0.32$, to capture the effects of water contaminants on the water surface reflective properties. All other parameters were fixed as specified at the start of Section 3.1. In addition, the glacier freezing temperature was fixed to its baseline value $T_c = -10^\circ\text{C}$.

The evolution of the system's equilibrium as α_w changes is illustrated as a bifurcation diagram in Figure 3. A stable (solid, blue) branch and a saddle (dotted, red) branch meet at a saddle point ($\alpha_w^* = 0.37$, with $\eta^* = 0.56$ and $w^* = -10.46$), marked with a green square. The iceline component of the stable equilibrium increases with decreasing α_w , and reaches the iceline top boundary value $\eta^+ = 1$ at $\alpha_w^+ = 0.31$ (with a temperature component of $w^+ = 7.98$). The iceline of the saddle equilibrium decreases with α_w reaches the boundary $\eta^- = 0$ at $\alpha_w^- = 0.13$ (with a temperature component of $w^- = -20.48$).

This results in the system only having access to the stable equilibrium for values of α_w in the interval $[\alpha_w^-, \alpha_w^+]$. When the albedo is not within this interval, the system approaches in the long-term either a water-covered Earth (for $\alpha_w < \alpha_w^-$), or a snowball Earth (for $\alpha_w > \alpha_w^+$).

With a nominal value of $\alpha_w = 0.32 \in [\alpha_w^-, \alpha_w^+]$, very small positive perturbations around this value may shrink the attraction basin of the stable equilibrium, and subsequently redirect some initial conditions originally converging to a high iceline, to instead converge to an ice-covered Earth. Larger positive perturbations, that transcend the critical bifurcation value α_w^* , would seal the ice-covered Earth as the only possible fate for the system. Negative perturbations past α_w^- would cause all initial states to converge to the ice-free Earth.

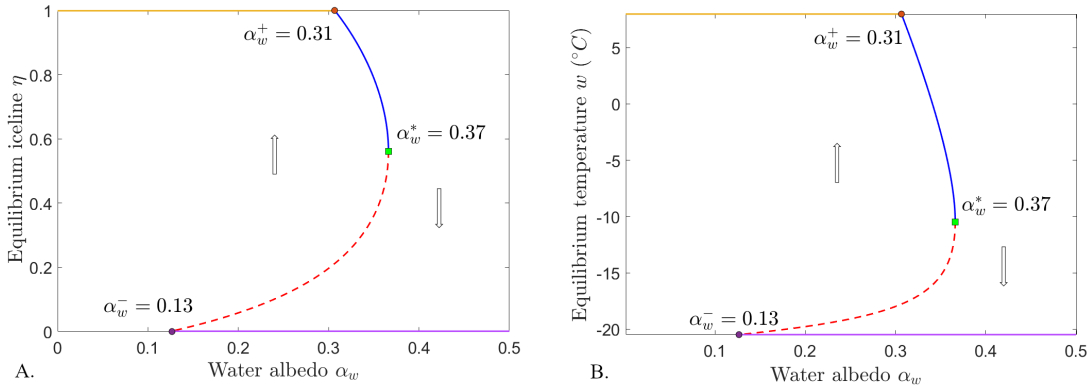


Figure 3: **Bifurcation of the system's equilibrium with respect to the water albedo α_w .** The panels show the evolution of the iceline component η (left) and of the temperature component w (right) of the equilibrium, as the parameter α_w changes. A locally stable branch (blue solid curve) and a saddle branch of the equilibrium (red dotted curve) collide at a saddle node bifurcation point at $\alpha_w = \alpha_w^*$, marked as a green square. The point where the stable equilibrium hits the upper iceline bound (at $\alpha_w = \alpha_w^+$) is marked with a brown dot. The iceline $\eta = 1$ (in the left panel) and the corresponding temperature ($w = w^+$, in the right panel) are marked as orange curves for $\alpha_w < \alpha_w^+$, since this boundary state now attracts all initial conditions in the region marked by the upward arrow. The point where the saddle equilibrium hits the lower iceline bound (at $\alpha_w = \alpha_w^-$) is marked with a purple dot. The iceline $\eta = 0$ (in the left panel) and the corresponding temperature ($w = w^-$, in the right panel) are marked as violet curves for $\alpha_w > \alpha_w^-$, since this boundary state now attracts all initial conditions in the region marked by the downward arrow.

3.1.3 Simultaneous dependence on α_w and T_c

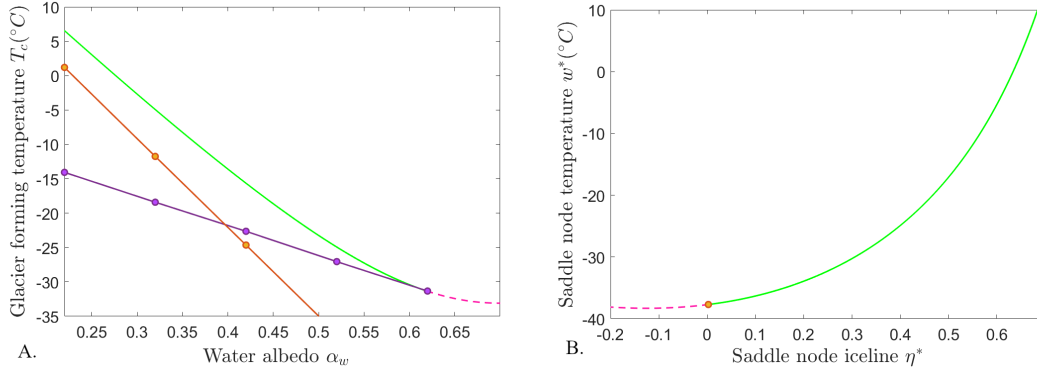


Figure 4: **Simultaneous dependence on α_w and T_c .** **A.** Bifurcations in the (α_w, T_c) parameter plane. The saddle node curve is shown as in green, within the physical domain $0 < \eta < 1$; it is extended as a pink dotted curve along a portion where the iceline $\eta < 0$). The parameter curve representing the intersection of the stable equilibrium with the top iceline boundary $\eta = 1$ is shown in brown. That representing the intersection of the saddle equilibrium with the bottom iceline boundary $\eta = 0$ is shown in purple. **B.** The phase plane components of the saddle node curve are shown, with the same color convention as in the left panel. The point where the iceline components becomes negative is marked with a brown dot.

The behavior of the equilibrium with respect to changes in the freezing temperature T_c is not unique for this parameter set. Since our discussion revolves around water quality, we can focus on tracking this behavior over the interval $[0,1]$ for the water albedo α_w . For different fixed values of α_w , the equilibrium curve with respect to T_c has qualitative the same U-shape, with two branches (a top, stable one and a bottom, unstable one) meeting at a saddle node bifurcation. However, the position of the saddle node changes, both in terms of the parameter value T_c^* and of the coordinates (η^*, w^*) corresponding to it. So does the value of T_c where the high (stable) equilibrium branch intersects the top iceline bound $\eta = 1$, and those where the low (unstable) equilibrium branch intersects the bottom iceline bound $\eta = 0$.

Figure 4a illustrates the evolution of the saddle node point (α_w^*, T_c^*) (with the corresponding evolution of the saddle node coordinates in the phase plane (η, w) being shown in Figure 4b). Notice that, as α_w increases and T_c decreases along the saddle node curve, the iceline value η^* declines, allowing for the possibility of lower and lower ice lines.

Figure 4a also shows the evolution of the collision point (α_w^+, T_c^+) of the equilibrium with the upper boundary $\eta = 1$ (orange curve) and the collision point (α_w^-, T_c^-) of the point with the lower boundary $\eta = 0$ (purple curve). The saddle node curve was computed and illustrated directly using the Matcont continuation software. For a good approximate illustration of the other two curves, the boundary points T_c^+ and T_c^- were extracted for five equilibrium curves (for $\alpha_w \in [0.22, 0.62]$, in 0.1 increments), and these sample points were interpolated by hand, as the orange and respectively purple curves.

Notice that the purple curve intersects the saddle node curve at $\alpha = 0.62$, $T_c = -31.3268$. For values of α here the saddle node exits the physical domain (which is very far from the current values of $\alpha_w = 0.32$ and $T_c = -10$). The thin, elongated parameter locus enclosed by these three curves (\mathcal{R}) represents the region of water purity where the system has access to a nontrivial long term iceline $0 < \eta^* < 1$. This gives a good representation of the effects of perturbations in water purity (as captured by the values of its albedo and its freezing temperature) from the current state

$\alpha_w = 0.32$, $T_C = -10$, which is inside the region \mathcal{R} . If the α_w and T_C are simultaneously increased, the system eventually exits \mathcal{R} across the saddle node bifurcation curve, and lands in the realm of the frozen Earth prognosis. If either α_w or T_C are decreased sufficiently, the system hits the brown curve, and access to the nontrivial iceline is replaced by access to the water-covered Earth (with the possibility of frozen Earth remaining available to certain initial conditions). If T_C is lowered while α_w is increased, the system hits the purple curve, and the water covered Earth becomes the only possible outcome.

3.2 Compounding greenhouse effects to water quality

In this section, we revisit the results in Section 3.1, examining their dependence on the parameter A , which encodes the strength of the greenhouse effect. This will allow us to better understand whether changes in water quality enhance the effects of climate change to the Earth’s long term dynamics.

3.2.1 Dependence on glacier forming temperature T_C

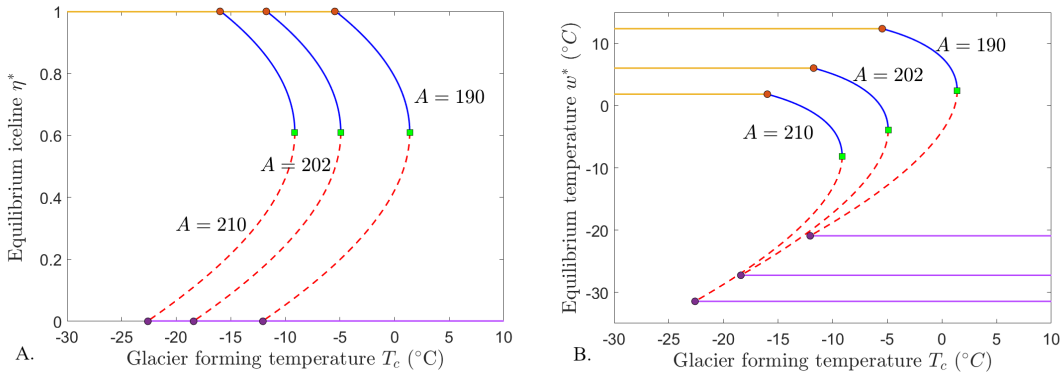


Figure 5: **Bifurcation of the system’s equilibrium with respect to the glacier forming temperature T_C , for different values of A .** The panels show the evolution of the iceline component η (left) and of the temperature component w (right) of the equilibrium, as the parameter T_C changes. Each different curve represents the evolution of the equilibrium for a different fixed value of the parameter A . In each case, a locally stable branch (blue solid curve) and a saddle branch of the equilibrium (red dotted curve) collide at a saddle node bifurcation point, marked as a green square. The point where the stable equilibrium curve hits the upper iceline boundary $\eta^+ = 1$ is marked with a brown dot, and the iceline and temperature corresponding to this extreme, ice-free Earth scenario, are shown for each A value as orange lines. The point where the saddle equilibrium curve hits the lower iceline boundary $\eta^- = 0$ is marked with a purple dot, and the iceline and temperature corresponding to this ice-covered Earth scenario, are shown as violet lines. The other parameters were fixed to the values in Table 1.

We want to explore to what extent greenhouse effects modulate the dependence of the system’s iceline dynamics on water purity (as reflected in the glacier forming temperature T_C). In our model increased greenhouse effects correspond to smaller values of the key parameter A . Hence, in Figure 5, we illustrate the system’s equilibrium behavior and bifurcations with respect to T_C , for three different values of A , corresponding to lower ($A = 210$), medium ($A = 202$) and higher ($A = 190$) concentrations of greenhouse gas in the atmosphere. The bifurcation diagram for each different A value is shown as a different curve. The evolution of the iceline (η^*) and temperature

(w^*) components of the equilibrium are shown separately in the left, and respectively in the right figure panel.

Notice that, for the A range represented here, all equilibrium curves exhibit a saddle node bifurcation (green square), marking the collision of a locally stable branch (blue curve) and a saddle branch (red curve) of the equilibrium. In each case, the stable equilibrium curve hits the upper iceline boundary at a parameter value T_c^+ , and the unstable equilibrium curve hits the lower iceline boundary at a parameter value T_c^- . As A decreases, the equilibrium curves (and subsequently the key points on these curves) shift to the right. More precisely, for $A = 190$, we have $T_c^+ = -5.4701$, $w^+ = 12.3790$; $T_c^- = -12.0602$, $w^- = -20.9288$; $T_c^* = 1.3900$, $\eta^* = 0.6092$, $w^* = 2.395$. For $A = 202$, we have $T_c^+ = -11.7468$, $w^+ = 6.0446$; $T_c^- = -18.4065$, $w^- = -27.2752$; $T_c^* = -4.9258$, $\eta^* = 0.6092$, $w^* = -3.9201$. For $A = 210$, we have $T_c^+ = -15.9831$, $w^+ = 1.8464$; $T_c^- = -22.5969$, $w^- = -31.4655$; $T_c^* = -9.1363$, $\eta^* = 0.6092$, $w^* = -8.1306$.

This means that freezing temperatures T_c which would lead to a snow cover Earth under low carbon conditions (higher A) may lead to a high iceline, or even to a completely water-covered Earth for high carbon conditions (lower A). Also notice that the temperature w corresponding to a water-covered Earth ($\eta = 1$) increases with higher carbon conditions.

Recall that the current freezing point T_c , leading to formation of glaciers, is $T_c = -10^\circ C$. Notice that for a small interval of high A values around 210, $T_c = -10$ is close to the saddle node T_c^* , hence a small variation in water purity negatively perturbing T_c may lead to placing the system on the left instead of the right side of the saddle node bifurcation, leading to a dramatically different long term outcome (high iceline versus ice covered Earth). When A is close to 205, small negative perturbations of T_c around the current value of $T_c = -10^\circ C$ may push a high iceline system into a regime where only the extremes (water covered or ice covered Earth) are possible, depending on initial conditions. For A even lower (close to 190), a small negative perturbation from $T_c = -10^\circ C$ may leave the water covered Earth as the only possible long term scenario.

3.2.2 Dependence on water albedo α_w

Figure 6 demonstrates the system's equilibrium behavior and bifurcations when changing the water albedo α_w , for the same three values of A as in the previous section ($A = 190$, $A = 202$ and $A = 210$). As before, each different curve corresponds to a different A values (as labeled); the evolution of the iceline component of the equilibrium is shown in the left panel, that of the temperature component is shown on the right.

All equilibrium curves exhibit a saddle node bifurcation (green square), where a stable (blue) and unstable (red) branches meet. The stable equilibrium branch hits the upper iceline boundary at $\alpha = \alpha^+$ (brown dots); the unstable equilibrium branch hits the lower iceline boundary at a parameter value α^- . As A decreases, the equilibrium curves shift to the right, as follows: for $A = 190$, we have $\alpha_w^+ = 0.3553$, with $w^+ = 7.2142$; $\alpha_w^- = 0.2737$, with $w^- = -19.2556$; $\alpha_w^* = 0.4266$, with $\eta^* = 0.4817$ and $w^* = -12.4236$. For $A = 202$, we have $\alpha_w^+ = 0.3066$, with $w^+ = 7.9847$; $\alpha_w^- = 0.1267$, with $w^- = -20.4856$; $\alpha_w^* = 0.3662$, with $\eta^* = 0.5613$ and $w^* = -10.4641$. For $A = 210$, we have $\alpha_w^+ = 0.2738$, with $w^+ = 8.5732$; $\alpha_w^- = 0.0298$ with $w^- = -21.2968$; $\alpha_w^* = 0.3278$, with $\eta^* = 0.6018$ and $w^* = -9.2382$.

Notice that water albedos α_w which would lead to a snow-covered Earth under low carbon conditions (higher A) may lead to a high iceline, or even to a completely water-covered Earth for high carbon conditions (lower A). Also notice that the temperature w corresponding to a water-covered Earth ($\eta = 1$) decreases with higher carbon conditions.

Notice that, for low carbon (A close to 210), the current water albedo $\alpha_w = 0.32$ is between the values α_w^+ and α_w^* , and close to both of these values. A small perturbation to higher albedo may lead to placing the system on the right instead of the left side of the saddle node bifurcation, leading to a dramatically different long term outcome (ice covered Earth versus high iceline). A

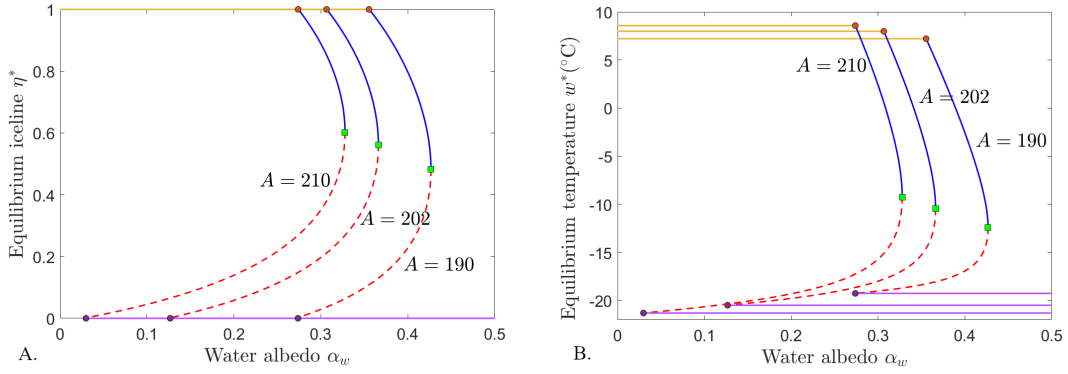


Figure 6: **Bifurcation of the system’s equilibrium with respect to the water albedo α_w , for different values of A .** The panels show the evolution of the iceline component η (left) and of the temperature component w (right) of the equilibrium, as the parameter α_w changes. Each different curve represents the evolution of the equilibrium for a different fixed value of the parameter A . In each case, a locally stable branch (blue solid curve) and a saddle branch of the equilibrium (red dotted curve) collide at a saddle node bifurcation point, marked as a green square. The point where the stable equilibrium curve hits the upper iceline boundary $\eta^+ = 1$ is marked with a brown dot, and the iceline and temperature corresponding to this extreme, ice-free Earth scenario, are shown for each A value as orange lines. The point where the saddle equilibrium curve hits the lower iceline boundary $\eta^- = 0$ is marked with a purple dot, and the iceline and temperature corresponding to this ice-covered Earth scenario, are shown as violet lines. The other parameters were fixed to the values in Table 1.

small negative perturbation of α_w may push a high iceline system into a regime where only the extremes (water covered or ice covered Earth) are possible, depending on initial conditions.

3.2.3 Simultaneous dependence on T_c and α_w

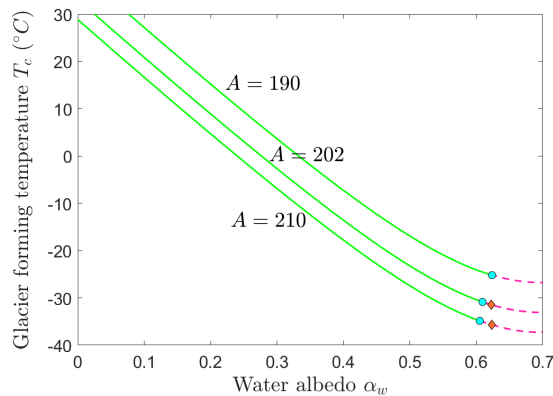


Figure 7: **Saddle-node bifurcation curves with respect to the albedo α_w , for different values of the greenhouse effect A .** The physical portion of each bifurcation curve (corresponding to iceline $0 \leq \eta^* \leq 1$) is shown in green; the portion corresponding to negative iceline is shown as a dotted pink continuation. The two scenarios are separated on each curve by a cyan dot. The pink diamond represents a cusp point, which always occurs in the negative iceline range.

To understand the simultaneous dependence of the system’s dynamics on freezing temperature and water albedo, one efficient approach is to separate the regions corresponding to different behaviors in the parameter plane (α_w, T_c) , and how this profile changes with different circumstances. In Section 3.1.3, our simulations identified a saddle-node curve for a fixed value of $A = 202$. This curve delimits a region of (α_w, T_c) values that may lead to a high iceline, or even a water-covered Earth (to the left of the curve) from a region of (α_w, T_c) in which only an ice-covered Earth is possible in the long-term (to the right of the curve). Our further computations show that is in fact representative for a larger range of A .

To illustrate the changes brought on by perturbations in A , Figure 7 shows the corresponding saddle-node curves in the plane (α_w, T_c) for three different A values. While these curves are very similar in shape, they visibly shift to the right as A is decreased. This suggests, in line with our intuition, that an increased greenhouse effect (lower A) increases the system’s long-term propensity for water versus ice.

4 Discussion

Significant prior research on the Budyko model with dynamic iceline has focused on the contribution of greenhouse effects to the evolution of the Earth’s climate system. In our study, we analyzed an extension of the Budyko model with dynamic iceline, centered around the impact of water quality (in conjunction with greenhouse effects) on the system’s long term dynamics. To do this, we considered two key parameters, both of which depend on different aspects of water purity: the glacier formation temperature T_c , and the albedo α_w .

First, we analyzed the system’s behavior under perturbations of each of these two parameters independently. When we examined the dependence on glacier forming temperature T_c , we found that the system undergoes a saddle node bifurcation with respect to this parameter, so that access to a high iceline stable equilibrium is only possible for a relatively small interval for T_c . For all values outside of this interval, the system either approaches a water-covered or snow-covered Earth. This suggests that even a small content of water impurities (which alter the freezing point T_c) may compound to a dramatic long-term effect. Since water salinity has a considerable effect on T_c , and since the salinity itself depends on the amount of planetary ocean water (i.e., on the position of the iceline), in our future work we plan to study how the predictions change if T_c is included not as a fixed parameter, but as an iceline-dependent system variable. [1]

When we analyzed the system’s dependence on water albedo α_w , we also identified the presence of a saddle-node bifurcation, relatively close to the currently measured value of α_w . This suggests that the contributions of water purity to the oceanic albedo augment the effect that small fluctuations in water purity may have to the Earth’s climate in the long-term. We observed, for example, that when α_w and T_c increase simultaneously, the equilibrium iceline decreases (leading to larger ice caps). Since water albedo has been empirically tied to the presence of clouds (which in turn depend on temperature, air pressure and other factors), in our ongoing research we are working on including the contribution of clouds by making the albedo temperature-dependent. [3]

Finally, we examined compounding greenhouse effects on water quality. T_c and α_w have changes that occur when variable A has different values. For example, we found that higher concentrations of greenhouse atmospheric gasses (a lower value for A), result in the potential for the Earth reaching the water-covered state at lower temperatures.

Overall, our analysis suggests the intriguing possibility that, in addition to the well-studied and known direct effects of greenhouse gasses accumulating in the Earth’s atmosphere, there may be an indirect aspect, coupled with the contribution of other factors pertinent to climate dynamics (such as water purity). Our results place increased emphasis on the idea that seemingly unrelated human-generated effects, each known to have a detrimental effect to the environment, may in fact

compound effects, and have dramatic consequences to the future and survival of life on our planet.

Acknowledgement

I would first like to thank my thesis advisor, Anca Rădulescu, who has shared invaluable guidance and feedback with me which pushed my work to the next level.

I would also like to thank Pat Sullivan and Alicia Ivan for this opportunity to complete my thesis, but also for all of the opportunities and experiences I was able to have within the Honors Program at SUNY New Paltz. I know I have gained ample knowledge that I will be able to take with me after graduation.

References

- [1] Nova online/cracking the ice age/greenhouse - green planet.
- [2] Lucas Benney and Anca Radulescu. An energy balance model of carbon's effect on climate change. *arXiv preprint arXiv:1512.07635*, 2015.
- [3] J.A. Coakley. Reflective and albedo, surface, 2003.
- [4] Willis Eschenbach. Of water and albedo, Aug 2018.
- [5] Shouting Gao, Xiaopeng Cui, and Xiaofan Li. A modeling study of relation between cloud amount and sst over western tropical pacific cloudy regions during toga coare. *Progress in Natural Science*, 19(2):187–193, 2009.
- [6] Richard McGehee and James Walsh. Climate modeling, dynamically speaking.
- [7] Lazaros Oreopoulos and Roger Davies. Statistical dependence of albedo and cloud cover on sea surface temperature for two tropical marine stratocumulus regions. *Journal of climate*, 6(12):2434–2447, 1993.
- [8] Jim Walsh and Richard McGehee. Modeling climate dynamically. *The College Mathematics Journal*, 44(5):350–363, 2013.
- [9] Esther Widiasih and Richard McGehee. A simplification of budyko's ice-albedo feedback model, 2012.